



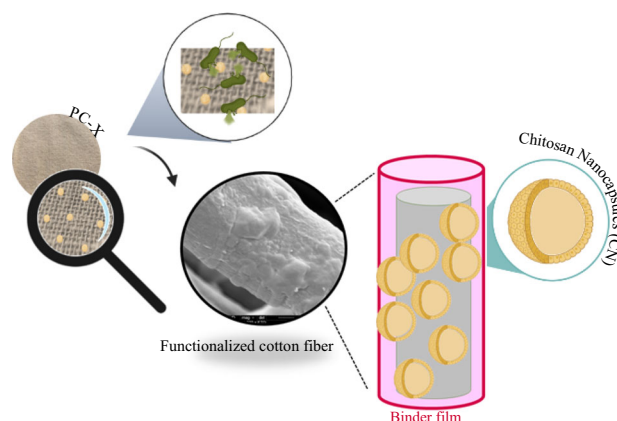
Multifunctional cotton fabrics with novel antibacterial coatings based on chitosan nanocapsules and polyacrylate

Daniel J. da Silva , Rafaela R. Ferreira, Greiciele da S. Ferreira, Rennan F. S. Barbosa, Jéssica S. Marciano, Paulo H. Camani, Alana G. Souza, Derval S. Rosa

Received: 21 August 2022 / Revised: 1 January 2023 / Accepted: 8 January 2023
© American Coatings Association 2023

Abstract Chitosan is a cationic polysaccharide with intrinsic antimicrobial properties that can be used as an ecological alternative to develop functional materials to inhibit the proliferation of microorganisms. This work evaluates chitosan nanocapsules (CNs) as a self-disinfecting agent to provide bactericidal activity on cotton fabrics (CF), using polyacrylate to bind the CNs on the CF surface. The fabrics were characterized by Fourier-transform infrared spectroscopy (FTIR), scanning electron microscopy (SEM), contact angle (CA), moisture retention, and antimicrobial tests against *Escherichia coli* and *Bacillus subtilis*. The FTIR results showed new peaks related to chitosan structure, indicating the adequate fixation of the CNs on the cotton fibers. SEM images corroborated the polyacrylate binder's efficient adhesion, connecting the CNs and the cotton fiber surface. The CF surface properties were considerably modified, while CN/polyacrylate coating promoted antibacterial activity against the *B. subtilis* (gram-positive bacteria) for the developed wipe, but they do not display bactericidal effects against *E. coli* (gram-negative bacteria).

Graphical abstract



Keywords Cotton, Chitosan, Antimicrobial, Multifunctional fabrics, Natural fibers

Introduction

Throughout human history, fabrics have had several cultural and technological functions, from participating in fashion and comfort to keeping the human body warm in cold climates, protecting from the sun in hot places, or protecting from microorganisms in highly contaminated places. In recent years, the textile industry has focused on improving the functional properties of fabrics, and there is a growing search for multifunctional wipes, which arose during the COVID-19 pandemic that highlighted a sanitary crisis.¹ Recent evidence suggests antimicrobial wipes are a good option for controlling bacterial pathogen proliferation on surfaces of clothes.² There have been significant efforts to meet the sanitary demands using

Supplementary Information The online version contains supplementary material available at <https://doi.org/10.1007/s11998-023-00761-y>.

D. J. da Silva, R. R. Ferreira, G. da S. Ferreira,
R. F. S. Barbosa, J. S. Marciano,
P. H. Camani, A. G. Souza,
D. S. Rosa (✉)

Center for Engineering, Modeling, and Applied Social Sciences (CECS), Federal University of ABC (UFABC), Av. dos Estados, Santo André, SP 5001 CEP 09210-210, Brazil
e-mail: dervalrosa@yahoo.com.br

promising and efficient materials to bring new functional properties to the textile sector.³ These new strategies have focused on using new green materials to functionalize cotton wipes to control several bacteria.⁴

Cotton fibers have several functional properties suitable for developing textiles, such as water absorbency, porosity, flexibility, and durability.⁵ Nowadays, the textile industry has been forced to meet new customer demands in addition to the basic functions of textiles (i.e., body protection and warmth). Self-cleaning, anti-fogging, anti-frosting, super-anti-wetting, antimicrobial, and UV-blocking are some of these novel multifunctional properties required by increasingly demanding customers.

Numerous materials have been investigated as promising antibacterial agents. Metals, such as zinc nanoparticles, copper, and silver, are widely used and recognized as efficient.^{6,7} However, these substances are commonly toxic, or their effects are unknown in the human organism, making them unsuitable for skin contact products.⁸ Therefore, numerous scientific efforts have been made to design new antimicrobial multifunctional textiles based on sustainable and natural antimicrobial agents, such as essential oils and chitosan.^{9–11} Chitosan (Cs) is a cationic polysaccharide derived from chitin, a polysaccharide composed of N-acetyl-D-glucosamine (GlcNAc) and mainly of D-glucosamine (GlcN).¹² The chitosan structure contains hydroxyls and amino groups that allow physical and chemical modifications, improving the crosslinking capacity. Besides, as chitosan is a cationic macromolecule, it has attracted considerable interest due to its biological activities.¹³ The positive charges on the chitosan surface result in strong electrostatic interactions with the cell surface, altering the cell permeability and leading to protein loss from the cytoplasm to the extracellular space.¹⁴ Studies have demonstrated antimicrobial activity against bacteria such as *Escherichia coli*, *Streptococcus mutans*, *Staphylococcus aureus*, *Bacillus subtilis*, and *Actinomyces naeslundii*.^{15,16}

One of the challenges of using chitosan in cotton wipes is washout durability.¹⁷ Since CNs cannot form covalent bonds with cotton fibers, they tend to slough off the fabric surface during the wash and wear processes. For this reason, there are still rare studies about using only natural organic particles on cotton fabrics to develop multifunctional textiles for antimicrobial applications. So, an effective chitosan immobilization on the fabric surface is crucial. This strategy to improve antibacterial fabric is studied in the present work, using polyacrylate as a nanocapsule/cotton fiber binder. Polyacrylates are salt or esters of acrylic acid with a wide application as adhesives and glues in several technological areas.¹⁸ Hebeish and collaborators¹⁹ showed that cotton fabrics functionalized with chitosan/polymethacrylic acid nanoparticles show activity against some bacteria when copper is complexed with chitosan macromolecules. Chitosan/polyacrylic acid nanocomposites were studied as an anticancer drug delivery system.²⁰ Chitosan-acrylate

nanogels with essential oils were applied as an insect repelling coating on cotton fabrics.²¹ However, published research about using CN/polyacrylate coatings to produce antimicrobial fabrics is out of the scope of our knowledge.

Herein, different concentrations of chitosan nanocapsules (CNs) were incorporated and immobilized on the cotton textile using a polyacrylate binding agent. The effect of multifunctional fabric with CNs/polyacrylate was investigated by several techniques, such as Fourier transform infrared spectroscopy (FTIR), scanning electron microscopy (SEM), water absorption, and contact angle. Furthermore, the antimicrobial activity of multifunctional textiles against different bacteria was evaluated and discussed.

Materials and methods

Materials

Cotton fabrics were acquired from a fabric store (São Paulo, Brazil). Polymar Indústria Comércio Importação e Exportação Ltda. supplied chitosan (degree of deacetylation of 82% and M_w of 1×10^5 g mol⁻¹). Aqueous acrylic copolymer binder (Res 180 W Binder water) was purchased from Redelease (São Paulo, Brazil). Nutrient culture medium (Mueller-Hilton agar) was purchased from Kasvi. The other chemicals were purchased from Labsynth Produtos para Laboratórios Ltda. (Diadema, SP, Brazil). Sodium tripolyphosphate (TPP) and Tween 80 were acquired from Synth (Brazil).

Methods

Synthesis of chitosan nanocapsules (CNs)

The preparation of chitosan nanocapsules (CNs) was prepared according to the methodology described in our previous work,²² and their complete characterization was also reported. Cs was dissolved in a 1% (v/v) acetic acid/distilled water solution. Subsequently, Tween 80 (0.3 wt%) was added to the Cs solution and stirred for 30 min. Finally, TPP solution (1 wt%) was slowly added to the chitosan solution under high stirring. CNs were formed in the emulsion via electrostatic crosslinking between amino groups of chitosan and phosphate groups of TPP. Posteriorly, CNs were extracted from the emulsion by centrifugation at 10,000 rpm for 5 min.

Preparation of chitosan/cotton fabrics

Pieces of pristine cotton fabrics (PC) (10 cm × 10 cm) were previously washed with an aqueous detergent solution. After that, they were dipped in 100 mL of liquor containing water with the binder (3% v/v) and

different emulsion concentrations of chitosan nanocapsules (1, 2, 4, and 8% v/v) previously homogenized in a mechanical rotor shaker for 3 min (50 Hz). Then, the cotton fabrics were left in the liquor at room temperature and shaken in a Dubnoff bath with reciprocal agitation (EL Labor Equipamentos para Laboratórios Ltda, Santo André, Brasil) for 60 min. Finally, the functionalized fabrics were air-dried at room temperature (72 h), washed in distilled water (3 times), and air-dried again. The samples were named PC-*X*, where *X* corresponds to the emulsion content of CNs applied in liquor. The schematic representation of the fabrication of the cotton wipes coated with CN/polyacrylate is illustrated in Fig. 1.

Characterization of the CN liquor

Dynamic light scattering (DLS)

The CN diameter distribution was recorded using the dynamic light scattering (DLS) technique with a 90° scattering angle using Zetasizer Nano-ZS equipment (Malvern Panalytical Ltd., Malvern, U.K.). The CN/polyacrylate liquor (100 μ L) was suspended in distilled water (2 mL), and each sample was analyzed in triplicate.

Zeta potential

The zeta potential was estimated by the Smoluchowski model from measurements of the electrophoretic mobility of the nanocapsules using Zetasizer Nano-ZS (Malvern Instruments). The reading time to obtain

the zeta potential data was 10 s, and the measurements were performed in triplicate.

Characterization of the CN/polyacrylate-cotton fabrics

X-ray photoelectron spectroscopy (XPS)

XPS measurements were performed using K-alpha⁺ equipment (ThermoFisher Scientific Inc., Massachusetts, USA), with monochromatic radiation Al K α , at 10 or 20 eV for high-resolution scans at room temperature.

Fourier-transform infrared spectroscopy

FTIR spectra were recorded in Frontier 94.942 (PerkinElmer Inc., Massachusetts, USA), operating with attenuated total reflectance (ATR). Data acquisition was performed in a range of 500–4000 cm^{-1} , 32 scans, and a spectral resolution of 4 cm^{-1} .

Scanning electron microscopy (SEM)

The samples were coated with a 25-nm-thick gold layer, using Sputtering Leica EM ACE 200 (Leica Microsystems, Wetzlar, Germany). Micrographs were performed using a microscope FEI Quanta 250 (Thermo Fisher Scientific, Hillsboro, Oregon, USA), using an accelerating voltage of 10 kV and a spot size of 4 nm.

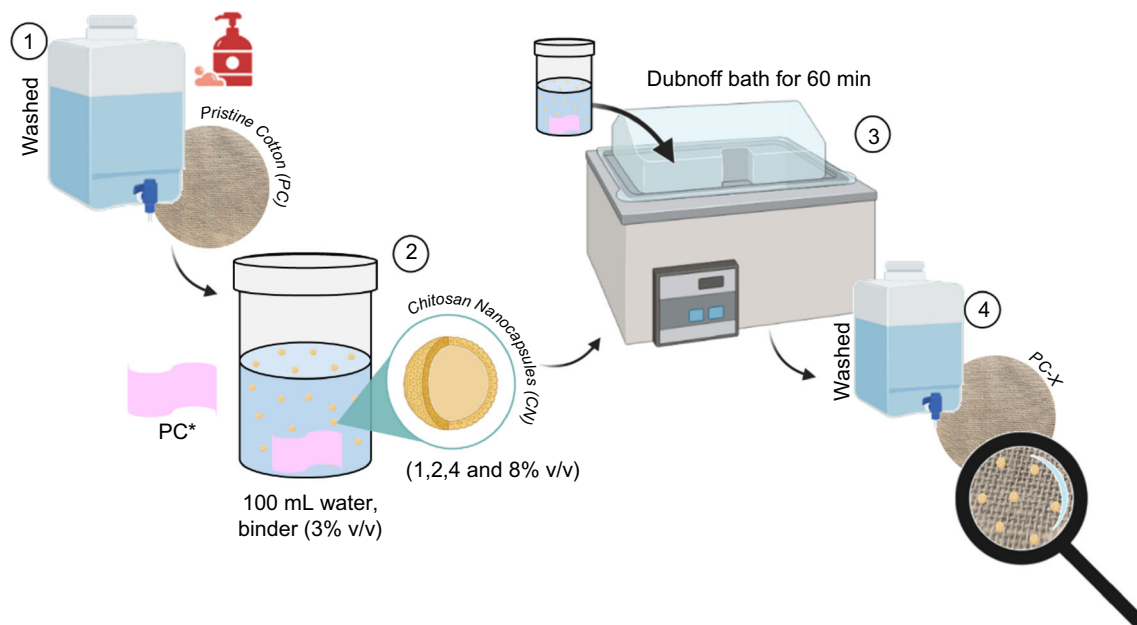


Fig. 1: Schematic representation of the adopted methodology. Chitosan/polyacrylate cotton fabrics were named PC-*X*, where *X* corresponds to the emulsion content of CN applied in liquor

Moisture retention

The moisture of the CN/polyacrylate-cotton fabrics was determined by the weight loss of the sample as a function of time. The samples were cut into $2 \times 2 \text{ cm}^2$ and dried in an oven at 60°C for 96 h. The experiments were performed in triplicate, and the weight of water retained by the cotton fabric was calculated using equation (1), where W_t is the weight of the sample at a time t , and W_{t0} is the moisture weight of the samples.

$$W\% = \frac{W_{t0} - W_t}{W_{t0}} \times 100 \quad (1)$$

Contact angle

The contact angle was measured using a dynamic contact angle tensiometer (SEO) model Phoenix 300 (Kromtech Alliance Corp., London, UK), with three phases (air/water/sample). The static contact angles (θ_{est}) were determined according to the Young–Laplace equation by observing sessile water droplets of $4.00 \mu\text{L}$ deposited on the cotton fabric's surface. The contact angle values were collected on the drop after 30 s in contact with the fabric's surface.

Water absorption rate (ϕ)

Φ was determined from the contact angle data. For this purpose, it was used as the water drop volume (V),²³ drop/sample interface area (A_θ) and time interval between the θ_{est} measurements (Δt_θ), according to equation (2).

$$\phi = \frac{V}{A_\theta \Delta t_\theta} = \frac{\pi h(3r^2 + h^2)/6}{\pi r^2 \Delta t_\theta} = \frac{h}{6\Delta t_\theta} \left(3 + \frac{h^2}{r^2} \right) \quad (2)$$

where h and r correspond to the height and water/sample interface radius of the sessile drop at the time t_θ . Using the Quincke relation [equation (3)] and equation (4),^{24,25} equation (5) was derived to estimate ϕ in the function of θ_{est} , water specific mass ($\rho = 1 \text{ g cm}^{-3}$), water surface tension ($\sigma = 72.8 \text{ mJ m}^{-2}$), and gravity ($g = 9.8 \text{ m s}^{-2}$).

$$h^2 = 2\sigma \frac{(1 - \cos\theta_{\text{est}})}{g\rho} \quad (3)$$

$$\frac{h}{r} = \tan\left(\frac{\theta_{\text{est}}}{2}\right) \quad (4)$$

$$\phi = \frac{1}{6\Delta t_\theta} \sqrt{2\sigma \frac{(1 - \cos\theta_{\text{est}})}{g\rho}} \left[3 + \tan\left(\frac{\theta_{\text{est}}}{2}\right) \right] \quad (5)$$

Antimicrobial tests

The antimicrobial test was performed using the bacterial growth inhibition method in nutrient broth. For this purpose, the cotton fabrics with different proportions of CN were cut in a square format with an area of 1 cm^2 and added to a test tube containing a nutrient culture medium inoculated with *Escherichia coli* (*E. coli*, ATCC 25922) or *Bacillus subtilis* (*B. subtilis*, Caron Beta A 155) (10^5 CFU mL^{-1}). The test tubes were kept for 24 h in a microbiological incubator at 30 and 37°C for bacterial growth of *E. coli* and *B. subtilis*, respectively. After incubation, the inoculated medium ($100 \mu\text{L}$) was plated into Petri dishes with nutrient agar by the spread plate method. Counting of microorganisms (in CFU mL^{-1}) was performed in Petri dishes after being incubated for 24 h at the same temperatures suitable for each bacterial strain. Bacterial inhibition corresponds to the difference between the logarithm of the number of bacterial colony-forming units (in CFU mL^{-1}) observed in the nutrient broth with the samples and that observed in the positive control (nutrient broth inoculated with bacteria at a count of 10^5 CFU mL^{-1} without direct contact with samples).

Statistical analysis

Two-way analysis of variance (ANOVA two-way) and Tukey's test were applied to statistically evaluate the significant differences between the samples' measured properties, using a 95% confidence level in the GraphPad Prism 7.

Results and discussion

CN/polyacrylate liquor

DLS and Zeta potential

The particle size distribution plots of the CNs are shown in Fig. 1S (Supplementary Material). The CN presents a hydrodynamic diameter (D_H) distribution with an average diameter of $100 \pm 10 \text{ nm}$, while the zeta potential (ζ) is $+16.5 \pm 5.1 \text{ mV}$ (Table 1). When CNs are introduced into the liquor containing water and the binder, the hydrodynamic diameters remain monomodal Gaussian profile distribution, but CN aggregates with D_H average from 50 to 410 nm are formed.

The binder may be responsible for the CN aggregation in the liquor since the protonated amine and hydroxyl groups of the chitosan chains can interact or react with carboxylic acids (COOH) present on polyacrylate,²⁶ a component of the acrylic binder, forming amide or ester linkages as illustrated in Fig. 2. In addition, the ζ values out of the range of $+30$ and -30 mV indicate that the aggregates have electrostatic charges to repulse each other and stabilize them in the

Table 1: Hydrodynamic diameter (D_H) and Zeta potential (ζ) of the chitosan nanocapsules (CNs) in the liquor

Sample	Hydrodynamic diameter distribution	Hydrodynamic diameter (nm)	Zeta potential (mV)
CN	Gauss distribution (Monomodal)	100 ± 10^{22}	$+16.5 \pm 5.1^{22}$
PC-1	Gauss distribution (Monomodal)	246 ± 172	-30.5 ± 6.9
PC-2	Gauss distribution (Monomodal)	222 ± 160	-36.2 ± 8.7
PC-4	Gauss distribution (Monomodal)	178 ± 116	-37.8 ± 5.5
PC-8	Gauss distribution (Monomodal)	209 ± 136	-36.9 ± 7.7

*PC-X, where X corresponds to the CN emulsion content applied in liquor

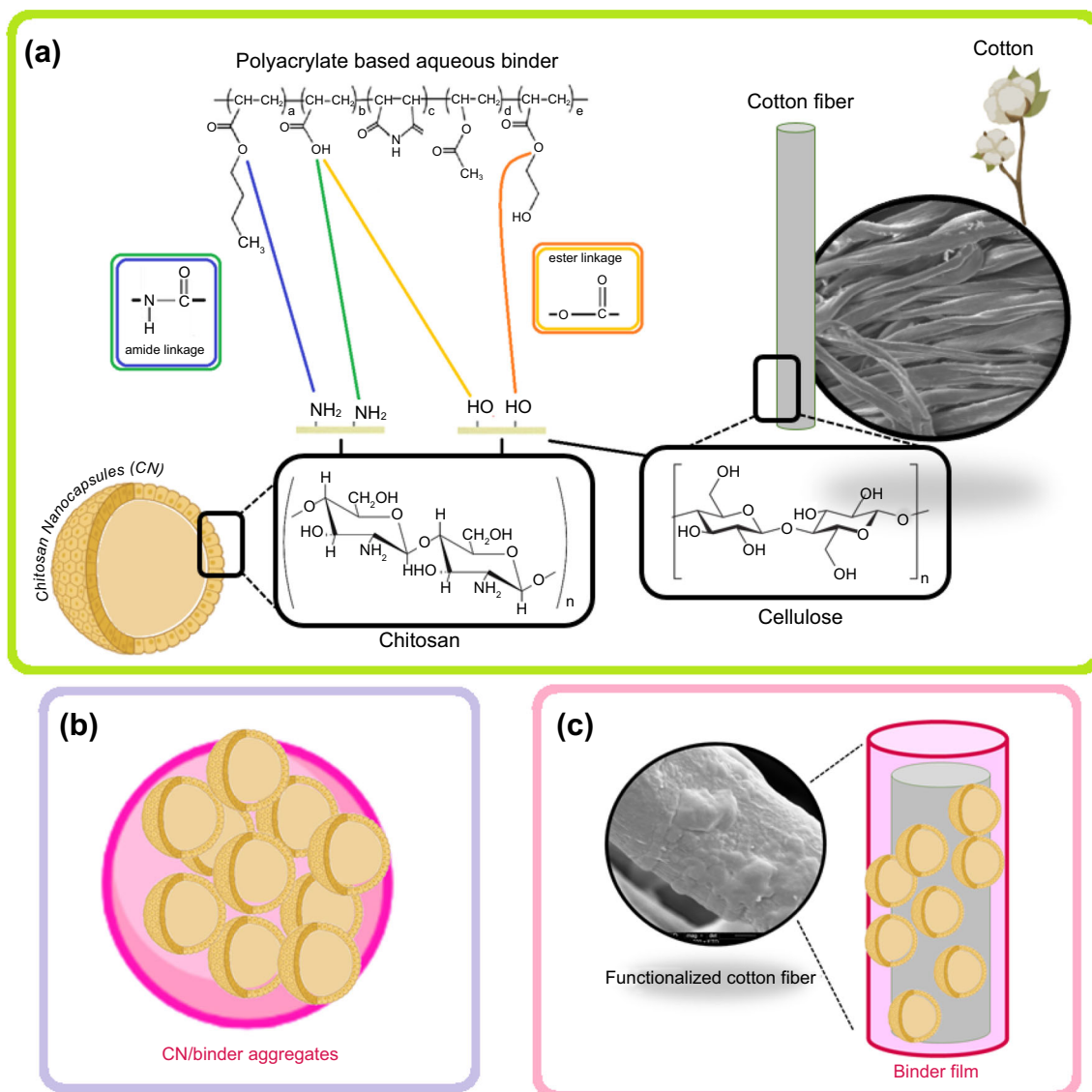


Fig. 2: (a) Ester ($-\text{OCO}-$) and amide ($-\text{NHCO}-$) bonds between chitosan nanocapsules (CN) and polyacrylate in the binder due to aminolysis (blue bar), condensation (green bar), transesterification (orange bar), and esterification (yellow bar). The binder fixes on the cotton fibers' surface also due to the reactions of hydroxyl (OH) groups on cellulose chains with ester and carboxylic acids on polyacrylate. These reactions also lead to the formation of (b) CN/binder aggregates, and (c) a binder film on the cotton fiber's surface with nanocapsules trapped inside (CN/polyacrylate coating)

aqueous medium.²⁷ The ionized COO⁻ groups of the polyacrylate binder forming a negative electrostatic layer covering the CN must cause repulsive forces to repel the CN aggregates of each other, as suggested by the high negative ζ average values (<-30 mV).

CN/polyacrylate-cotton fabrics

XPS spectroscopy

The PC sample presents XPS binding energies at 399.9 eV (N–C=O amide bonds, N_{1s} region), 284.5 eV (C–C and C–H bonds, C_{1s} region), 285.9 eV (C–O bonds, C_{1s} region), 287.4 eV (C–O–C bonds, C_{1s} region), 288.1 eV (N–C=O bonds, C_{1s} region), 289.3 eV (O–C=O bonds, C_{1s} region), 531.1 eV (OH bonds, O_{1s} region), 533.6 eV (O–C bonds, O_{1s} region), 532.3 eV (C–O–C bonds, O_{1s} region), and 534.9 eV (water, O_{1s} region) associated with the cellulose, proteins, and waxes present on the cotton fabrics.²⁸ The XPS signals at 289.3 eV and 532.5 eV in the C_{1s} and O_{1s} XPS spectra indicate the presence of COOH chemical groups^{28–30} on the cotton fibers due to their bleaching treatment,³¹ as shown in Fig. 3a.

The polyacrylate binder presents XPS signals indicated in Fig. 3b at 284.6 eV (C–C and C–H bonds, C_{1s} region), 285.0 eV (C–O bonds, C_{1s} region), 288.6 eV (O–C=O bonds, C_{1s} region), 286.5 eV (C–NH bonds, C_{1s} region), 399.4 eV (C–NH–C bonds, N_{1s} region), 288.6 eV (O–C=O bonds, C_{1s} region), 531.8 eV (OH bonds, O_{1s} region), 533.3 eV (C–O and C=O bonds, O_{1s} region), 532.3 eV (C–O–C bonds, O_{1s} region), and 534.5 eV (O–C=O bonds, O_{1s} region) confirming the chemical linkages in the binder illustrated in Fig. 2.^{32–34}

The XPS spectra from the PC-8 sample (CN/polyacrylate-cotton fabric) in Fig. 3c confirm the amide and ester chemical bonds between the polyacrylate and the chitosan forming the CN aggregates evidenced by DLS. Also, it confirms the presence of CNs on the cotton fabric's surface due to the N_{1s} XPS spectra at 399.8 eV (N–C=O bonds), 401 eV (C–NH–C bonds), and 398.5 eV (C–NH₂ bonds).^{32–34} Moreover, the XPS signal intensity at 288.6 eV (O–C=O bonds, C_{1s} region) and 534.3 eV (O–C=O bonds, O_{1s} region) from ester linkages is a contribution of the OH groups on cellulose chains reactions with the carboxylic acids on polyacrylate responsible for the CNs fixation on the cotton fibers' surface.

Fourier-transform infrared spectroscopy

The pristine cotton fabrics present a typical spectrum of cellulose type I (Fig. 4a) with characteristic peaks at 3300–3000 cm⁻¹ (OH groups), 2890 cm⁻¹ (CH₂ stretching vibration), 1638 cm⁻¹ (OH vibrations from absorbed water), 1425 cm⁻¹ (CH₂ scissoring at C(6)), 1362 cm⁻¹ (CH bending), 1338 and 1201 cm⁻¹ (OH in-plane bending), 1162 cm⁻¹ (C–O–C asymmetric

stretching), 1103, 1060, and 1032 cm⁻¹ (C–O stretching), and 895 cm⁻¹ (C–O vibration of cellulose type I).³⁵ After the chitosan nanocapsules addition, a new peak appeared at 1728 cm⁻¹ (Fig. 4b) assigned to the amide I band of chitosan.³⁶ Besides, the shoulder at 1452 cm⁻¹ turned into a new low-intensity peak attributed to C–H bending on chitosan carbon structure,³⁷ confirming the effective fixation of CN on the cotton fibers.

The PC crystallinities were investigated by FTIR-ATR using different methods to evaluate the effect of the binder or chitosan on the fibers' surface. The crystallinity measured by FTIR is used to evaluate cellulose qualitative changes based on the ratio of absorbance bands at specific wavenumbers. It is a technique used to compare samples submitted to the same treatment or characteristics.^{38,39} The first methodology was proposed by Zhang et al.⁴⁰ According to the authors, the peak height of 2900 cm⁻¹/2850 cm⁻¹ can be used to verify the presence of wax in cellulosic samples, named wax crystallinity index (WCI). Based on the fitting curves (Figs. 4c–4g), the obtained values are presented in Table 2. This method considers the bands 2950 and 2850 cm⁻¹, assigned to CH₂ asymmetrical and symmetrical stretching of alkyl groups of waxes in the cellulose cuticle.⁴¹ The results indicated that all samples show high WCI; as the ATR is a technique that mainly detects the sample surface, a high wax content is expected in all fibers, mainly for PC and PC-1, which can be a result of both cellulose pectin and lignin naturally present in cotton fibers.^{40,42} The samples with high chitosan nanocapsules showed lower WCI values, confirming the binder presence in functional wipes.

Two other methods were used to evaluate the crystallinity of cotton wipes using the FTIR-ATR qualitatively. The first presented method was proposed by Nelson and O'Connor that measures the lateral order index (LOI) by the ratio between 1427 cm⁻¹/898 cm⁻¹ bands,^{39,43} and low values reflect a disordered structure. After that, Nelson and O'Connor developed a new measurement method based on the ratio between 1372 cm⁻¹/2900 cm⁻¹, defined as total crystallinity index (TCI).^{43,44}

The crystallinity order for methods I, II, and III is practically identical. The lateral order index represents the ordered regions perpendicular to the cellulose chain direction, which is greatly influenced by chemical processes. The LOI values indicate a large portion of amorphous cellulose,⁴⁵ similar to all the samples and without significant changes after the binder addition. Besides, this value is also affected by water absorption, and the cellulose crystallinity decreases with fiber swelling; for this reason, these results are doubtful, and other methodologies are often presented together.

The TCI value, according to Nelson and O'Connor, is a method that does not suffer the influence of absorbed water onto cellulose, and for this reason, it is considered an adequate method to evaluate the cellulose crystallinity.^{43,46} The TCI results indicate that few

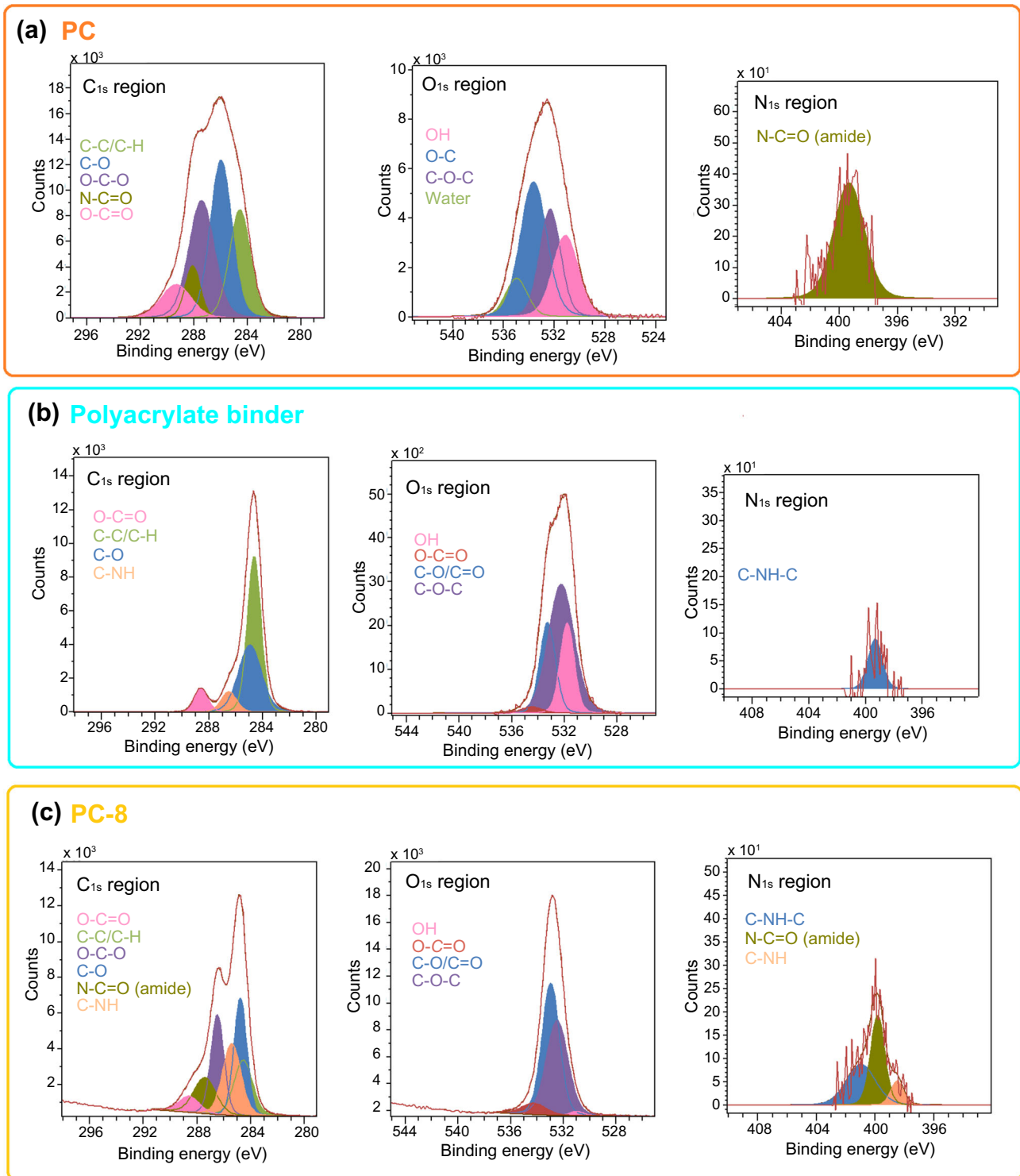


Fig. 3: XPS spectra in the C_{1s}, O_{1s}, and N_{1s} binding energy regions from pristine cotton fabric (a), polyacrylate binder (b), and CN/polyacrylate-cotton PC-8 sample (c)

OH- groups are available to interact by inter- and/or intramolecular hydrogen bondings on cotton fiber even with the chitosan/polyacrylate coating.⁴⁷

Scanning electron microscopy (SEM)

Figure 5 presents SEM images for pristine cotton fabric (PC) and fabrics containing different CN contents (PC-

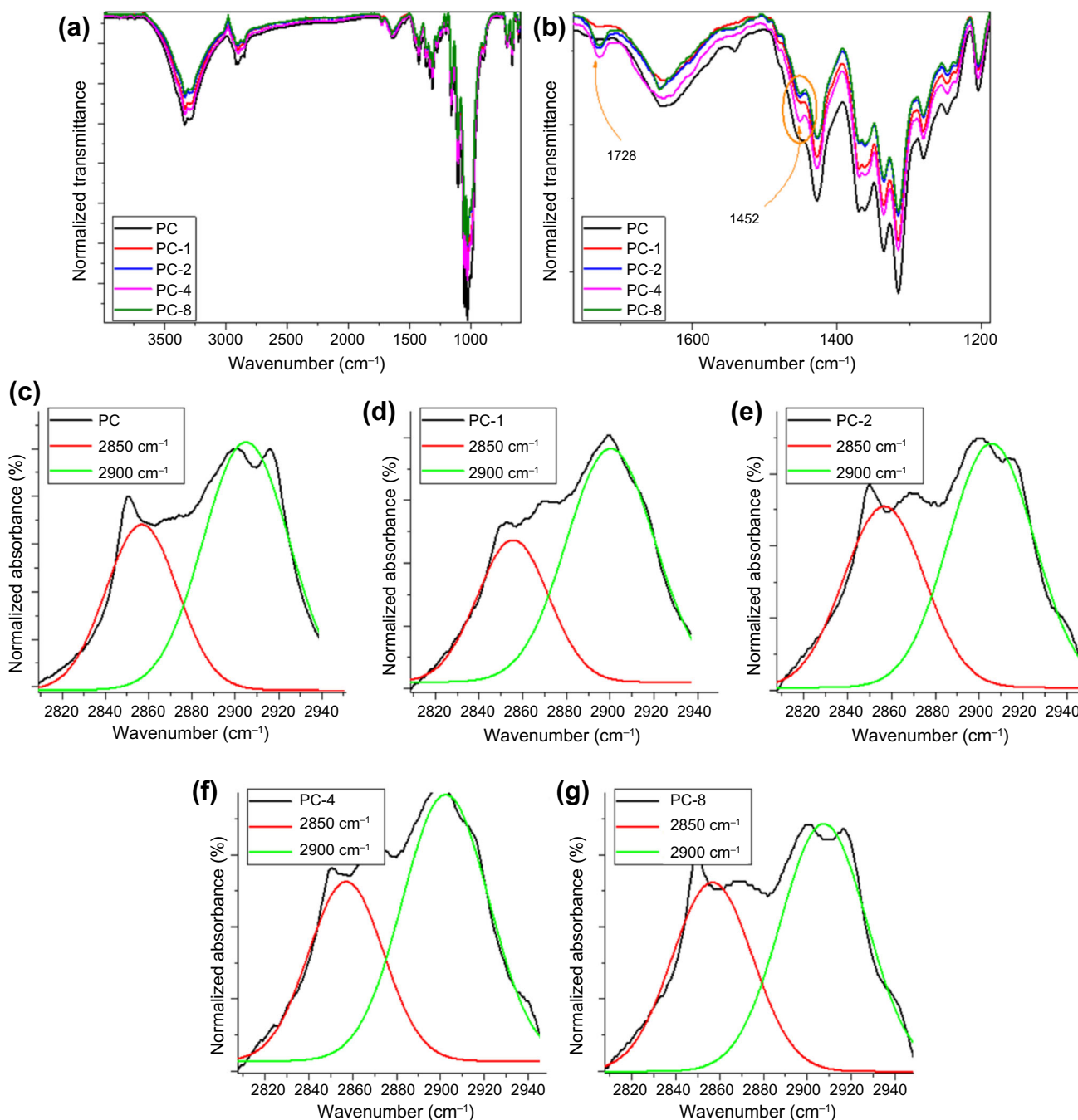


Fig. 4: FTIR spectra of pristine cotton (PC) and PC-X, where X corresponds to the chitosan nanocapsules content. (a) Full spectra and (b) zoom in the region 1750–1200 cm^{-1} . Gauss fitting curves of the spectra in the 2850 and 2900 cm^{-1} peaks of the samples: (c) PC, (d) PC-1, (e) PC-2, (f) PC-4, and (g) PC-8

X). Firstly, the PC sample presented the characteristic morphology of cotton fabrics and their fibers, with a regular surface, without defects and apparent roughness. Untreated cotton fabrics' morphology was also observed by Zhang and co-workers and Ferreira and co-workers.^{48,49}

With the addition of chitosan nanocapsules, some aggregates of capsules may be observed on the fiber's surface, as observed in Fig. 5b (PC-1), suggesting that the interaction between cotton fibers chitosan capsules well-fixed the particles at the fibers' surface. Thus, the presence of nanocapsules and binder (same in low

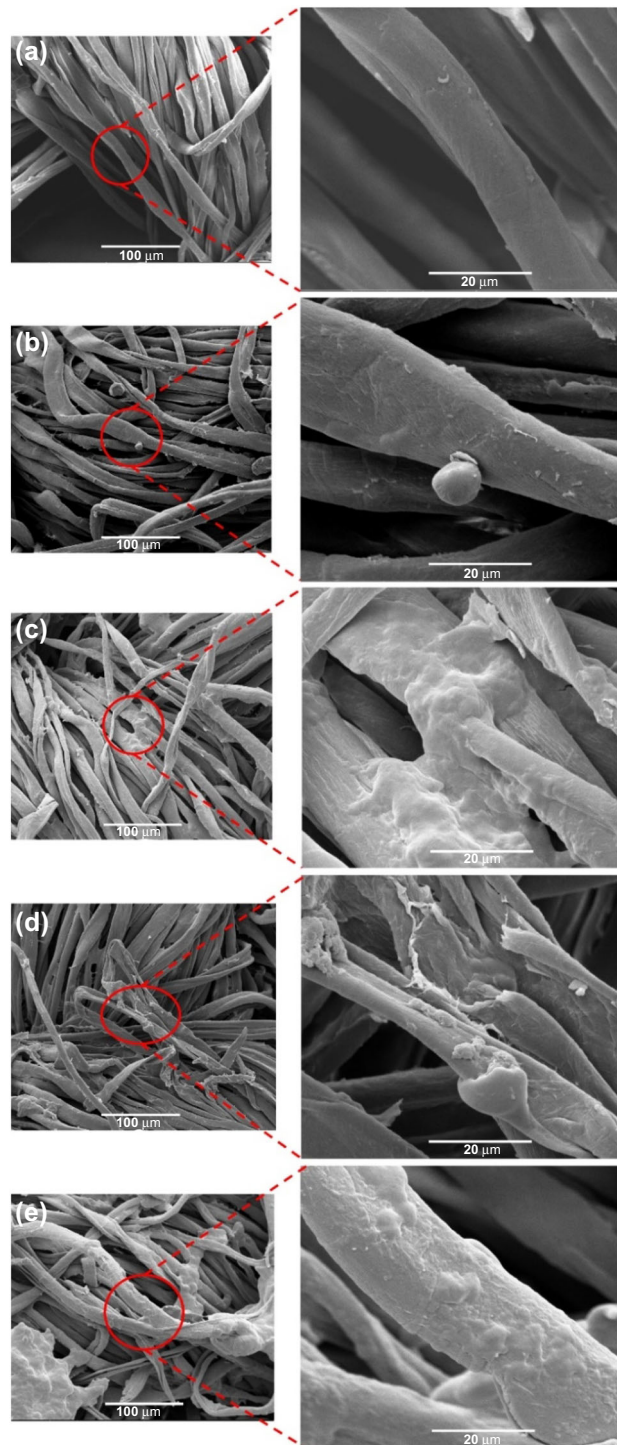


Fig. 5: SEM micrographs of cotton fabrics before and after they had been treated with different contents of chitosan nanocapsule: (a) untreated, (b) PC-1, (c) PC-2, (d) PC-4, and (e) PC-8. The corresponding right-hand micrographs were taken at higher magnification. PC-X, where X corresponds to the chitosan nanocapsule content

concentrations) promoted interaction with cotton fibers, altering hydrodynamic diameter and zeta potential (ζ), adhering capsules on fiber's surface, and promoting dispersion. Ghayempour and Mortazavi

observed that acrylate binder provided interaction between alginate nanocapsules containing peppermint oil and fiber's surface.⁵⁰

Table 2: Wax crystallinity index (WCI) and cellulose crystallinity measurements by FTIR using different absorbance ratios: lateral order index (LOI) and total crystallinity index (TCI)

Sample	WCI: 2900 cm ⁻¹ /2850 cm ⁻¹	LOI: 1427 cm ⁻¹ /898 cm ⁻¹	TCI: 1372 cm ⁻¹ /2900 cm ⁻¹
PC	0.9	0.2	0.9
PC-1	1.0	0.2	1.0
PC-2	0.8	0.2	0.9
PC-4	0.9	0.2	0.9
PC-8	0.8	0.2	0.9

According to the increase of chitosan nanocapsules on CN/polyacrylate liquor (especially Figs. 5c, 5d, and 5e, respectively), cotton fabrics presented one dense layer of other material. One hypothesis is the agglomeration of chitosan nanocapsules due to high interaction with polyacrylate binder (Fig. 2), promoting strong linkages between these structures, resulting in a dense layer on the fiber’s surface. Sun and Iqbal observed similar considerations since higher nanocapsule and binder concentrations generate the system’s saturation, thus generating agglomerates.⁵¹ Therefore, the polyacrylate binder provided interaction between chitosan nanocapsules and cotton fiber’s surface; however, higher concentrations resulted in agglomeration due to the system’s saturation, compromising an adequate dispersion of the capsules on the surface of the cotton fiber.

Contact angle

The textile wettability was investigated using the contact angle measurements, and the result is presented in Fig. 6. The initial contact angle was compared with the value after 30 s to understand the impact of chitosan nanocapsules on fabrics’ surface properties. For pristine cotton (PC sample), an initial angle of 84.4° was observed, presenting a hydrophobic nature, which was expected since the fabrics are composed of cellulosic materials that exhibit surface hydroxyl groups as indicated in FTIR analysis.³⁵ Notably, the contact angle presented slight variation, reducing to 83.7° after 30 s which was unexpected since Patil and co-workers observed that cotton fabrics were completely wetted with time.⁵² This variation may arise from previous treatments of the obtained fabric, leaving residual material that impacted the surface properties.

After incorporating chitosan nanocapsules, some slight variation in the initial contact angle measurement was observed, related to the treatment employed. Additionally, the contact angle value after 30 s was highly impacted, showing a decrease with time. The variation depended on the loading of chitosan nanocapsules, where higher loadings promoted a higher variation in the contact angle.

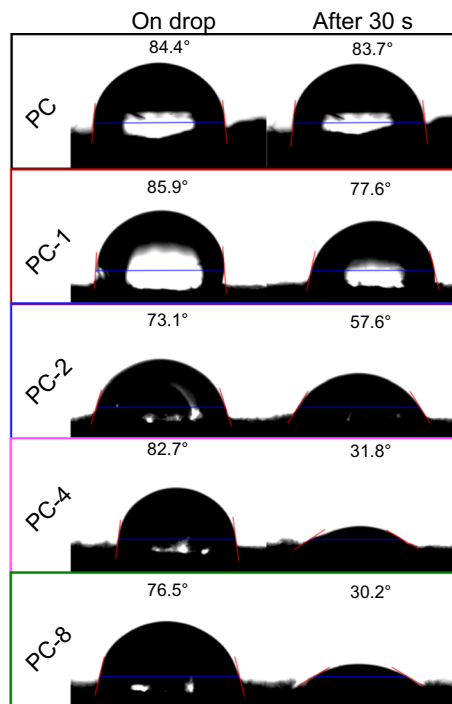


Fig. 6: Contact angle measurement on a drop and after 30 s of pristine cotton (PC) and PC-X, where X corresponds to the chitosan nanocapsule content

These observations indicate that the fabric’s surface was considerably impacted and corroborated SEM results indicated an additional layer over the fiber’s surface. This layer possibly results from the polyacrylate binder and chitosan nanocapsules, and since both materials present polar groups in their structure, the fabric’s surface properties became more hydrophilic with the binding of nanocapsules.²⁶ These findings are in accordance with the lowest difference between the Hildebrand solubility parameters (δ) of water ($\delta_{\text{water}}=47.8 \text{ MPa}^{1/2}$) and chitosan ($\delta_{\text{chitosan}}=46.3 \text{ MPa}^{1/2}$) than that for water and cellulose ($\delta_{\text{cellulose}}=42.1 \text{ MPa}^{1/2}$),^{53–55} indicating more affinity for water with the CN-cotton fibers with the increasing of CN content to improve the sessile water drop spreading and absorption onto the surface of the sample, as well as capillary

effects. As a result, the water drop absorption rate calculated from the contact angle measurements are 0.8 (PC), 8.8 (PC-1), 15.5 (PC-2), 49.9 (PC-4), and $44.8 \mu\text{g m}^2 \text{s}^{-1}$ (PC-8). This proposed method is suitable to compare the water absorption rate of the cotton textiles before and after the surface treatment and evaluate the ease of spreading of water by the fabric that is a phenomenon essential to ensure that the moisture coming from the skin evaporates easily, giving a dry feeling effect and maintaining the user's comfort. An advantage of this method is that the absorption rate is little affected by the water saturation absorbed by the fabrics since the measurement is performed in a local micrometric area. Raja et al.⁵⁶ point out such interference in different methods suggested by them to estimate the water absorbency rate of fabrics based on different materials, including cotton.

Moisture retention

The ability of the cotton fabric to absorb a certain amount of moisture from the air is known to affect other textile properties, such as heat transport, electrical conductivity, swelling, the perceived comfort of clothing, and especially microbial activity.^{57,58} The excess moisture in the textile fabric promotes bacteria and fungi growth, causing mold and mildew.^{59,60} It is important to evaluate the impact of the content of chitosan capsules on the moisture retention of cotton fabrics. Figure 2S shows the moisture retention studies for PC and PC-X. All the samples containing chitosan nanocapsules presented rapid moisture loss, reaching a plateau in the first hour. The moisture loss retained in the fabric was lowest for the PC-2 sample (5.09 w/w %), followed by PC-8, PC-4, and PC-1, obtaining moisture content levels of 5.38, 6.61, and 7.59 w/w %, respectively (Table 3). Already, the PC sample showed a slower rate of moisture loss, reaching equilibrium after 48 h and a moisture loss of 7.59 w/w %.

The crosslinked chitosan nanocapsules act as impermeable domains, providing a lower moisture retention capacity to the cotton fabric and achieving equilibrium with the relative humidity of the environment faster.^{61,62} CN/binder coating reduces the moisture absorption capacity of the fabrics with capsules following the free volume theory. Although chitosan has a high affinity with water, according to Hildebrand solubility parameters, a large amount of crosslinking bonds like chitosan/triphosphate/chitosan in the nanocapsules and chitosan/polyacrylate/chitosan in the CN/binder film lead to a reduction in the free volume inside the CN/binder film. So then, the high crosslinking degree inhibits the water adsorbed molecules from permeating into the cotton fibers and occupying the interior of the CN or CN/binder film. Although hydrogen bonds are expected to form between the hydroxyl groups and amines groups, the fibers achieve an equilibrium with the relative humidity

of the environment faster with the increase of CN content since a significant water content remains adsorbed onto the surface of the PC-X samples with CN.

Antimicrobial tests

From the antimicrobial tests (Figs. 7a and 7c), only the PC-8 sample presents significant bactericidal activity against *S. subtilis* (Gram-positive, G+) after 24 h of direct contact with the bacterial broth, which can be explained by the highest amount of CNs in the chitosan/polyacrylate coating. All samples do not display significant antimicrobial performance against *E. coli* (Gram-negative, G-), as shown in Figs. 7b and 7d. The outstanding bacterial effect from PC-8 corroborates the literature, as some studies report damage to bacterial membrane cells as chitosan concentrations increase.⁶³

These antimicrobial results of the CN/polyacrylate cotton fabrics against the G- strain indicate that *E. coli* are less susceptible to the presence of NH_2 and COOH groups on the fabric surface, which are responsible for their bactericidal activity when they are electrically charged after ionization forming NH_3^+ and COO^- .³¹ When ionized, they can chelate and abstract cations from the surface of the outer cell membrane that cover the *E. coli* cell wall, such as Mg^{2+} and K^+ , causing an electrostatic unbalance of the bacterial membrane and, consequently, the extensive membrane rupture, compromising the bacteria cell activities. The amino groups are crucial to chitosan's antibacterial mechanism because the positively charged chitosan interacts with the negatively charged bacterial cell surface, causing lysis (leakage into the cell). Polycationic chitosan interacts with the structure of lipopolysaccharides and proteins present in bacterial cell walls.⁶⁴ The protonation of amino groups increases the degree of electrostatic repulsion and polarity along the chitosan chain.⁶⁵

In addition to affecting the outside of bacterial cells, polymeric chitosan chains with a molar mass of less than $5 \times 10^6 \text{ g mol}^{-1}$ can penetrate the cytoplasm and cell nucleus of bacteria and bind to DNA, preventing mRNA synthesis and, consequently, production of proteins inherent in the gene translation process.^{64,66} Therefore, the bactericidal effect against *S. subtilis* of the PC-8 sample is directly connected with the surface chemistry of this G+ strain, whose membrane is predominantly negatively charged due to the presence of phosphate groups present in teichoic acids (components of the lipopolysaccharide cell wall), being essential to stabilize this layer through electrostatic interactions with cations.⁶⁷ In addition, the cationic Cs can chelate with the metal cations present on the G+ bacteria cell (Mg^{2+} and Ca^{2+}) wall causing extensive disruption of the peptidoglycan layer and possible bacterial cell lysis.⁶⁸

E. coli is a bacteria strain with an outer membrane composed of lipopolysaccharides (LPS), lipoproteins,

Table 3: The time for total moisture loss and total moisture weight retained by pure cotton (PC) and PC-X, where X corresponds to the CN content

Sample	Moisture loss (w/w %)	Time for total moisture loss (min)
PC	7.59±0.01	2880
PC-1	7.59±0.01	15
PC-2	5.09±0.01	15
PC-4	6.61±0.01	15
PC-8	5.38±0.01	30

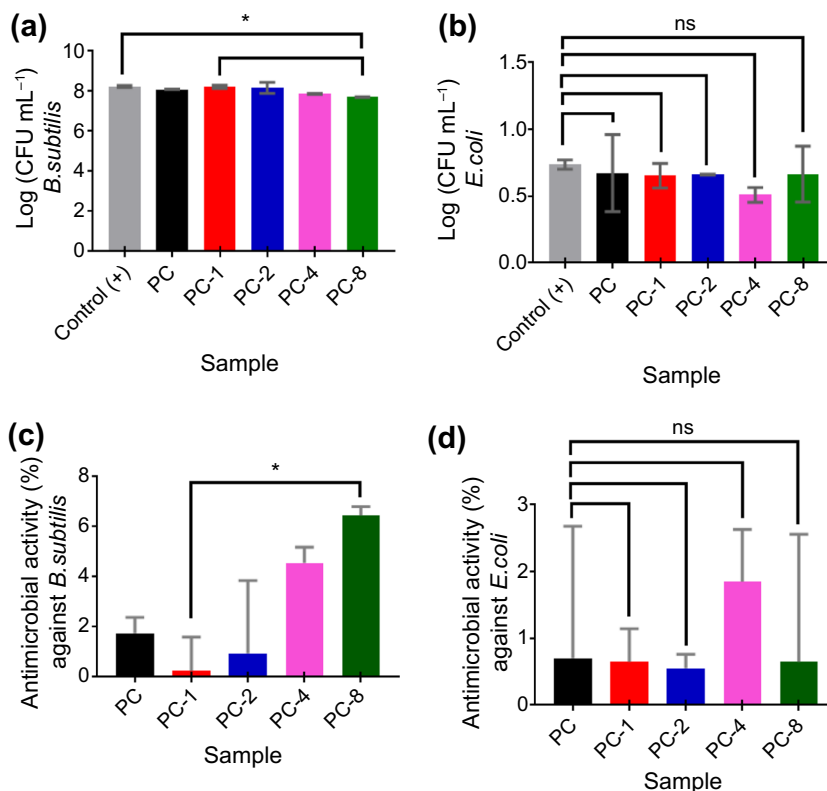


Fig. 7: Bacterial counting and antimicrobial activity of uncoated cotton fabric (PC) and PC-X samples (X corresponds to the CN content) after 24 h of direct contact with the bacterial medium: (a, c) *B. subtilis* and (b, d) *E. coli*. The values are presented as mean±standard deviation. *Samples are statistically different, considering a confidence level of 95%. ns= samples are not statistically different, considering a confidence level of 95%

and phospholipids covering the peptidoglycan cell layer. According to the literature, G- bacteria are surrounded by negatively charged lipopolysaccharides, making them quickly attracted to charged amino groups.³¹ However, this electrostatic communication between glucosamine amino groups (positively charged) and the *E. coli* cell membranes (negatively charged) seems to be slightly effective due to the possible low amount of NH₂ groups accessible on the CN/polyacrylate cotton fabrics. Such interactions would compromise the integrity of the outer bacteria membrane, altering the electrochemical potential gradients through the ion channels in the bacterial cell walls and leading to changes in a bacterial barrier and intracellular permeability, preventing the entry of

essential nutrients into the cell and occasioning the bacterial cell lysis. The antimicrobial results further suggest that interactions by London forces between CN and the cytoplasmic membrane phospholipids of G-bacteria, which would also cause cell damage of this G-bacteria, also seem to have no significant effect on inhibiting bacterial growth of *E. coli* in the CN concentrations investigated in this work.

Conclusions

Antimicrobial cotton fabrics containing different CN concentrations for use in bactericidal wipes have been

successfully obtained. The FTIR results indicated that the treatment preserved cotton structure and new peaks related to chitosan structure were observed, suggesting the CN presence at the fibers' surface. SEM images and XPS spectra showed the efficient adhesion of the polyacrylate binder, connecting the CNs on the cotton fiber surface. Fabrics' wettability was investigated after incorporating the CN. A slight variation in the measurement of the initial contact angle concerning the treatment used was observed, indicating that the variation depended on the loading of the CN, whose higher loads promoted a more significant variation in contact angle. The moisture content was evaluated, and modified cotton fabrics reached equilibrium with the relative humidity of the environment faster with the increase in the CN content. Finally, the surface of the coated fabrics shows bactericidal activity against *S. subtilis* (G+) for high CN concentrations (PC-8), but not against *E. coli* (G-). This study indicates the potential applicability of cotton fabrics containing chitosan nanocapsules using a simple coating procedure to develop eco-friendly antimicrobial wipes, using high CN loading in the CN/polyacrylate coatings.

Acknowledgments This research was funded by Fundação de Amparo à Pesquisa do Estado de São Paulo (2022/01382-3, 2021/14714-1, 2021/08296-2, 2020/13703-3 and 2019/16301-6), Conselho Nacional de Desenvolvimento Científico e Tecnológico (308053/2021-4 and 403934/2021-4), and CAPES-Pandemias (8881.504639/2020-01). The authors thank the CAPES (Code 001), REVALORES Strategic Unit, and MULTIUSER CENTRAL FACILITIES (UFABC).

Data availability The data supporting this study's findings are available from the corresponding author upon reasonable request.

References

- Wesgate, R, Robertson, A, Barrell, M, Teska, P, Maillard, J-Y, "Impact of Test Protocols and Material Binding on the Efficacy of Antimicrobial Wipes." *J. Hosp. Infect.*, **103** e25–e32. <https://doi.org/10.1016/j.jhin.2018.09.016> (2019)
- Siani, H, Wesgate, R, Maillard, J-Y, "Impact of Antimicrobial Wipes Compared with Hypochlorite Solution on Environmental Surface Contamination in a Health Care Setting: A Double-Crossover Study." *Am. J. Infect. Control.*, **46** 1180–1187. <https://doi.org/10.1016/j.ajic.2018.03.020> (2018)
- Mohamed, AL, El-Naggar, ME, Hassabo, AG, "Preparation of Hybrid Nanoparticles to Enhance the Electrical Conductivity and Performance Properties of Cotton Fabrics." *J. Mater. Res. Technol.*, **12** 542–554. <https://doi.org/10.1016/j.jmrt.2021.02.035> (2021)
- El-Nahhal, IM, Salem, J, Anbar, R, Kodeh, FS, Elmanama, A, "Preparation and Antimicrobial Activity of ZnO-NPs Coated Cotton/Starch and Their Functionalized ZnO-Ag/Cotton and Zn(II) Curcumin/Cotton Materials." *Sci. Rep.*, **10** 5410. <https://doi.org/10.1038/s41598-020-61306-6> (2020)
- Abou Elmaaty, T, Elsisy, HG, Elsayad, GM, Elhadad, HH, Sayed-Ahmed, K, Plutino, MR, "Fabrication of New Multifunctional Cotton/Lycra Composites Protective Textiles Through Deposition of Nano Silica Coating." *Polymers (Basel)*, **13** 2888. <https://doi.org/10.3390/polym13172888> (2021)
- Dadi, R, Azouani, R, Traore, M, Mielcarek, C, Kanaev, A, "Antibacterial Activity of ZnO and CuO Nanoparticles Against Gram Positive and Gram Negative Strains." *Mater. Sci. Eng. C*, **104** 109968. <https://doi.org/10.1016/j.msec.2019.109968> (2019)
- Thi Ngoc Dung, T, Nang Nam, V, Thi Nhan, T, Ngoc, TTB, Minh, LQ, Nga, BTT, Phan Le, V, Viet Quang, D, "Silver Nanoparticles as Potential Antiviral Agents Against African Swine Fever Virus." *Mater. Res. Express*, **6** 1250g9. <https://doi.org/10.1088/2053-1591/ab6ad8> (2020)
- Subramaniam, VD, Prasad, SV, Banerjee, A, Gopinath, M, Murugesan, R, Marotta, F, Sun, X-F, Pathak, S, "Health Hazards of Nanoparticles: Understanding the Toxicity Mechanism of Nanosized ZnO in Cosmetic Products." *Drug Chem. Toxicol.*, **42** 84–93. <https://doi.org/10.1080/01480545.2018.1491987> (2019)
- Yilmaz-Atay, H, "Antibacterial Activity of Chitosan-Based Systems." In: Jana, S, Jana, S (eds.) *Functional Chitosan*, pp. 457–489. Springer Singapore, Singapore (2019)
- Parvinzadeh, M, Memari, N, Shaver, M, Katozian, B, Ahmadi, S, Ziadi, I, "Influence of Ultrasonic Waves on the Processing of Cotton with Cationic Softener." *J. Surfactants Deterg.*, **13** 135–141. <https://doi.org/10.1007/s11743-009-1158-y> (2010)
- Jiang, X, Tang, X, Zhang, B, He, L, Shi, Y, "Antimicrobial Activity and Synergistic Antibacterial Mechanism of a Combination of Zinc and Rare-Earth Scandium Against *Escherichia coli*." *Mater. Technol.*, **35** 797–806. <https://doi.org/10.1080/10667857.2019.1688534> (2020)
- Si, Z, Hou, Z, Vikhe, YS, Thappeta, KRV, Marimuthu, K, De, PP, Ng, OT, Li, P, Zhu, Y, Pethe, K, Chan-Park, MB, "Antimicrobial Effect of a Novel Chitosan Derivative and Its Synergistic Effect with Antibiotics." *ACS Appl. Mater. Interfaces*, **13** 3237–3245. <https://doi.org/10.1021/acsmi.0c20881> (2021)
- Karoyo, AH, Wilson, LD, "A Review on the Design and Hydration Properties of Natural Polymer-Based Hydrogels." *Materials (Basel)*, **14** 1095. <https://doi.org/10.3390/ma14051095> (2021)
- Perinelli, DR, Fagioli, L, Campana, R, Lam, JKW, Baffone, W, Palmieri, GF, Casettari, L, Bonacucina, G, "Chitosan-Based Nanosystems and Their Exploited Antimicrobial Activity." *Eur. J. Pharm. Sci.*, **117** 8–20. <https://doi.org/10.1016/j.ejps.2018.01.046> (2018)
- Lin, M-H, Wang, Y-H, Kuo, C-H, Ou, S-F, Huang, P-Z, Song, T-Y, Chen, Y-C, Chen, S-T, Wu, C-H, Hsueh, Y-H, Fan, F-Y, "Hybrid ZnO/Chitosan Antimicrobial Coatings with Enhanced Mechanical and Bioactive Properties for Titanium Implants." *Carbohydr. Polym.*, **257** 117639. <https://doi.org/10.1016/j.carbpol.2021.117639> (2021)
- Varma, R, Vasudevan, S, "Extraction, Characterization, and Antimicrobial Activity of Chitosan from Horse Mussel *Modiolus modiolus*." *ACS Omega*, **5** 20224–20230. <https://doi.org/10.1021/acsomega.0c01903> (2020)
- Ranjbar-Mohammadi, M, "Production of Cotton Fabrics with Durable Antibacterial Property by Using Gum Traga-

- canth and Silver.” *Int. J. Biol. Macromol.*, **109** 476–482. <https://doi.org/10.1016/j.ijbiomac.2017.12.093> (2018)
18. Gardeen, S, Hylwa, S, “A Review of Acrylates: Super Glue, Nail Adhesives, and Diabetic Pump Adhesives Increasing Sensitization Risk in Women and Children.” *Int. J. Women’s Dermatol.*, **6** 263–267. <https://doi.org/10.1016/j.ijwd.2020.04.007> (2020)
 19. Hebeish, A, Sharaf, S, Farouk, A, “Utilization of Chitosan Nanoparticles as a Green Finish in Multifunctionalization of Cotton Textile.” *Int. J. Biol. Macromol.*, **60** 10–17. <https://doi.org/10.1016/j.ijbiomac.2013.04.078> (2013)
 20. Amini-Fazl, MS, Mohammadi, R, Kheiri, K, “5-Fluorouracil Loaded Chitosan/Polyacrylic Acid/Fe₃O₄ Magnetic Nanocomposite Hydrogel as a Potential Anticancer Drug Delivery System.” *Int. J. Biol. Macromol.*, **132** 506–513. <https://doi.org/10.1016/j.ijbiomac.2019.04.005> (2019)
 21. Kala, S, Agarwal, A, Sogan, N, Naik, SN, Nagpal, BN, Patanjali, PK, Kumar, J, “Chitosan-Acrylate Nanogel for Durable Anti Mosquito Finishing of Cotton Fabric and Its Dermal Toxicity Profiling on Swiss Albino Mice.” *Colloids Surfaces B Biointerfaces.*, **181** 789–797. <https://doi.org/10.1016/j.colsurfb.2019.06.022> (2019)
 22. Ferreira, RR, Souza, AG, Rosa, DS, “Essential Oil-Loaded Nanocapsules and Their Application on PBAT Biodegradable Films.” *J. Mol. Liq.*, **337** 116488. <https://doi.org/10.1016/j.molliq.2021.116488> (2021)
 23. Fan, CF, Cağın, T, “Wetting of Crystalline Polymer Surfaces: A Molecular Dynamics Simulation.” *J. Chem. Phys.*, **103** 9053–9061. <https://doi.org/10.1063/1.470016> (1995)
 24. Behroozi, F, Behroozi, PS, “Reliable Determination of Contact Angle from the Height and Volume of Sessile Drops.” *Am. J. Phys.*, **87** 28–32. <https://doi.org/10.1119/1.5078512> (2019)
 25. da Silva, JPP, Veras, MM, Leite, JYP, “Determinação de ângulo de contato usando aparato didático.” In: *II Congr. Pesqui. e Inovação Da Rede Norte Nord. Educ. Tecnológica*, João Pessoa, PB, 2007, pp. 1–6
 26. Farion, IA, Burdukovskii, VF, Kholkhoev, BC, Timashev, PS, Chailakhyan, RK, “Functionalization of Chitosan with Carboxylic Acids and Derivatives of Them: Synthesis Issues and Prospects of Practical Use: A Review.” *Express Polym. Lett.*, **12** 1081–1105. <https://doi.org/10.3144/expresspolymlett.2018.95> (2018)
 27. Naduparambath, S, Jinitha, TV, Shaniba, V, Sreejith, MP, Balan, AK, Purushothaman, E, “Isolation and Characterisation of Cellulose Nanocrystals from Sago Seed Shells.” *Carbohydr. Polym.*, **180** 13–20. <https://doi.org/10.1016/j.carbpol.2017.09.088> (2018)
 28. da Silva, DJ, da Silva Barbosa, RF, de Souza, AG, Ferreira, RR, Camani, PH, Nantes-Cardoso, IL, Rosa, DS, “Bactericidal Activity of Cotton Fabrics Functionalized by ZnO and Cu via Microwave.” *Cellulose*, **28** 8153–8175. <https://doi.org/10.1007/s10570-021-03990-9> (2021)
 29. Li, Z, He, Z, Chen, X, Tang, Y, You, S, Chen, Y, Jin, T, “Preparation of Hydrophobically Modified Cotton Filter Fabric with High Hydrophobic Stability Using ARGET-ATRP Mechanism.” *RSC Adv.*, **9** 24659–24669. <https://doi.org/10.1039/C9RA04123K> (2019)
 30. Mauger, O, Westphal, S, Klöpzig, S, Krüger-Genge, A, Müller, W, Storsberg, J, Bohrisch, J, “Plasma Activation as a Powerful Tool for Selective Modification of Cellulose Fibers Towards Biomedical Applications.” *Plasma*, **3** 196–203. <https://doi.org/10.3390/plasma3040015> (2020)
 31. Mahat, MM, Sabere, ASM, Azizi, J, Amdan, NAN, “Potential Applications of Conducting Polymers to Reduce Secondary Bacterial Infections Among COVID-19 Patients: A Review.” *Emergent Mater.*, **4** 279–292. <https://doi.org/10.1007/s42247-021-00188-4> (2021)
 32. Zhou, A, Li, L, Li, M, Chen, Q, “Fabrication of Poly(amide-co-ester) Solvent Resistant Nanofiltration Membrane from P-nitrophenol and Trimethyl Chloride via Interfacial Polymerization.” *Separations*, **9** 28. <https://doi.org/10.3390/separations9020028> (2022)
 33. Lozano-Montante, J, Garza-Hernández, R, Sánchez, M, Moran-Palacio, E, Niño-Medina, G, Almada, M, Hernández-García, L, “Chitosan Functionalized with 2-Methylpyridine Cross-Linker Cellulose to Adsorb Pb(II) from Water.” *Polymers (Basel)*, **13** 3166. <https://doi.org/10.3390/polym13183166> (2021)
 34. Prabhakar, MN, Raghavendra, GM, Vijaykumar, BVD, Patil, K, Seo, J, Jung-il, S, “Synthesis of a Novel Compound Based on Chitosan and Ammonium Polyphosphate for Flame Retardancy Applications.” *Cellulose*, **26** 8801–8812. <https://doi.org/10.1007/s10570-019-02671-y> (2019)
 35. Muzaffar, S, Bhatti, IA, Zuber, M, Bhatti, HN, Shahid, M, “Synthesis, Characterization and Efficiency Evaluation of Chitosan-Polyurethane Based Textile Finishes.” *Int. J. Biol. Macromol.*, **93** 145–155. <https://doi.org/10.1016/j.ijbiomac.2016.08.068> (2016)
 36. Chauhan, N, Dilbaghi, N, Gopal, M, Kumar, R, Kim, K-H, Kumar, S, “Development of Chitosan Nanocapsules for the Controlled Release of Hexaconazole.” *Int. J. Biol. Macromol.*, **97** 616–624. <https://doi.org/10.1016/j.ijbiomac.2016.12.059> (2017)
 37. Costa, EM, Silva, S, Veiga, M, Baptista, P, Tavaría, FK, Pintado, ME, “Textile Dyes Loaded Chitosan Nanoparticles: Characterization, Biocompatibility and Staining Capacity.” *Carbohydr. Polym.*, **251** 117120. <https://doi.org/10.1016/j.carbpol.2020.117120> (2021)
 38. O’connor, RT, Dupré, EF, Mitcham, D, “Applications of Infrared Absorption Spectroscopy to Investigations of Cotton and Modified Cottons: Part I: Physical and Crystalline Modifications and Oxidation.” *Text. Res. J.*, **28** 382–392. <https://doi.org/10.1177/004051755802800503> (1958)
 39. Hurtubise, FG, KrÄSSIG, H, “Classification of Fine Structural Characteristics in Cellulose by Infrared Spectroscopy Use of Potassium Bromide Pellet Technique.” *Anal. Chem.*, **32** 177–181. <https://doi.org/10.1021/ac60158a010> (1960)
 40. Zhang, L, Li, X, Zhang, S, Gao, Q, Lu, Q, Peng, R, Xu, P, Shang, H, Yuan, Y, Zou, H, “Micro-FTIR Combined with Curve Fitting Method to Study Cellulose Crystallinity of Developing Cotton Fibers.” *Anal. Bioanal. Chem.*, **413** 1313–1320. <https://doi.org/10.1007/s00216-020-03094-6> (2021)
 41. Abidi, N, Cabrales, L, Hequet, E, “Fourier Transform Infrared Spectroscopic Approach to the Study of the Secondary Cell Wall Development in Cotton Fiber.” *Cellulose*, **17** 309–320. <https://doi.org/10.1007/s10570-009-9366-1> (2010)
 42. He, Z, Nam, S, Fang, DD, Cheng, HN, He, J, “Surface and Thermal Characterization of Cotton Fibers of Phenotypes Differing in Fiber Length.” *Polymers (Basel)*, **13** 1–15. <https://doi.org/10.3390/polym13070994> (2021)
 43. Nelson, ML, O’Connor, RT, “Relation of Certain Infrared Bands to Cellulose Crystallinity and Crystal Lattice Type. Part II. A New Infrared Ratio for Estimation of Crystallinity in Celluloses I and II.” *J. Appl. Polym. Sci.*, **8** 1325–1341. <https://doi.org/10.1002/app.1964.070080323> (1964)
 44. Krüer-Zerhusen, N, Cantero-Tubilla, B, Wilson, DB, “Characterization of Cellulose Crystallinity After Enzymatic Treatment Using Fourier Transform Infrared Spectroscopy (FTIR).” *Cellulose*, **25** 37–48. <https://doi.org/10.1007/s10570-017-1542-0> (2018)

45. Kljun, A, Benians, TAS, Goubet, F, Meulewaeter, F, Knox, JP, Blackburn, RS, “Comparative Analysis of Crystallinity Changes in Cellulose I Polymers Using ATR-FTIR, X-ray Diffraction, and Carbohydrate-Binding Module Probes.” *Biomacromolecules*, **12** 4121–4126. <https://doi.org/10.1021/bm201176m> (2011)
46. Abidi, N, Manike, M, “X-ray Diffraction and FTIR Investigations of Cellulose Deposition During Cotton Fiber Development.” *Text. Res. J.*, **88** 719–730. <https://doi.org/10.1177/0040517516688634> (2018)
47. Široký, J, Blackburn, RS, Bechtold, T, Taylor, J, White, P, “Attenuated Total Reflectance Fourier-Transform Infrared Spectroscopy Analysis of Crystallinity Changes in Lyocell Following Continuous Treatment with Sodium Hydroxide.” *Cellulose*, **17** 103–115. <https://doi.org/10.1007/s10570-009-9378-x> (2010)
48. Ferreira, ILS, Medeiros, I, Steffens, F, Oliveira, FR, “Cotton Fabric Bleached with Seawater: Mechanical and Coloristic Properties.” *Mater. Res.*, **22** 1–8. <https://doi.org/10.1590/1980-5373-mr-2019-0085> (2019)
49. Zhang, Y, Yu, L, Ke, S, Shen, B, Meng, X, Huang, H, Lv, F, Xin, JH, Chan, HLW, “TiO₂/SiO₂ Hybrid Nanomaterials: Synthesis and Variable UV-Blocking Properties.” *J. Sol-Gel Sci. Technol.*, **58** 326–329. <https://doi.org/10.1007/s10971-010-2395-2> (2011)
50. Ghayempour, S, Mortazavi, SM, “Microwave Curing for Applying Polymeric Nanocapsules Containing Essential Oils on Cotton Fabric to Produce Antimicrobial and Fragrant Textiles.” *Cellulose*, **22** 4065–4075. <https://doi.org/10.1007/s10570-015-0765-1> (2015)
51. Sun, D, Iqbal, K, “Synthesis of Functional Nanocapsules and Their Application to Cotton Fabric for Thermal Management.” *Cellulose*, **24** 3525–3543. <https://doi.org/10.1007/s10570-017-1326-6> (2017)
52. Patil, GD, Patil, AH, Jadhav, SA, Patil, CR, Patil, PS, “A New Method to Prepare Superhydrophobic Cotton Fabrics by Post-coating Surface Modification of ZnO Nanoparticles.” *Mater. Lett.*, **255** 126562. <https://doi.org/10.1016/j.matlet.2019.126562> (2019)
53. García, JI, García-Marín, H, Pires, E, “Glycerol Based Solvents: Synthesis, Properties and Applications.” *Green Chem.*, **16** 1007–1033. <https://doi.org/10.1039/C3GC41857J> (2014)
54. Hansen, CM, *Hansen Solubility Parameters A User's Handbook*, 2nd edn. CRC Press (2007)
55. Ghorani, B, Russell, SJ, Goswami, P, “Controlled Morphology and Mechanical Characterisation of Electrospun Cellulose Acetate Fibre Webs.” *Int. J. Polym. Sci.*, **2013** 1–12. <https://doi.org/10.1155/2013/256161> (2013)
56. Raja, D, Ramakrishnan, G, Babu, VR, Senthilkumar, M, Sampath, M, “Comparison of Different Methods to Measure the Transverse Wicking Behaviour of Fabrics.” *J. Ind. Text.*, **43** 366–382. <https://doi.org/10.1177/1528083712456054> (2014)
57. Gao, Y, Zhu, G, Zhu, H, An, W, Xia, Y, “Experimental Study of Moisture Content Effects on Horizontal Flame Spread over Thin Cotton Fabric.” *Text. Res. J.*, **89** 3189–3200. <https://doi.org/10.1177/0040517518807450> (2019)
58. Belliveau, RG, DeJong, SA, Boltin, ND, Lu, Z, Cassidy, BM, Morgan, SL, Myrick, M, “Mid-infrared Emissivity of Nylon, Cotton, Acrylic, and Polyester Fabrics as a Function of Moisture Content.” *Text. Res. J.*, **90** 1431–1445. <https://doi.org/10.1177/0040517519888825> (2020)
59. Souza, JM, Henriques, M, Teixeira, P, Fernandes, MM, Figueiro, R, Zille, A, “Comfort and Infection Control of Chitosan-Impregnated Cotton Gauze as Wound Dressing.” *Fibers Polym.*, **20** 922–932. <https://doi.org/10.1007/s12221-019-9053-2> (2019)
60. Saha, J, Mondal, MIH, “Antimicrobial Textiles from Natural Resources: Types, Properties and Processing.” In: Mondal, MIH (ed.) *Antimicrobial Textiles from Natural Resources*, pp. 1–43. Elsevier. <https://doi.org/10.1016/B978-0-12-821485-5.00016-0> (2021)
61. Ta, Q, Ting, J, Harwood, S, Browning, N, Simm, A, Ross, K, Olier, I, Al-Kassas, R, “Chitosan Nanoparticles for Enhancing Drugs and Cosmetic Components Penetration Through the Skin.” *Eur. J. Pharm. Sci.*, **160** 105765. <https://doi.org/10.1016/j.ejps.2021.105765> (2021)
62. Yin, X, Weng, P, Han, L, Liu, J, Tan, Y, Chen, D, Zhou, Y, Li, S, Wang, L, Wang, H, “Enhanced Wettability and Moisture Retention of Cotton Fabrics Coated with Self-Suspended Chitosan Derivative.” *Cellulose*, **25** 2721–2732. <https://doi.org/10.1007/s10570-018-1707-5> (2018)
63. Chandrasekaran, M, Kim, KD, Chun, SC, “Antibacterial Activity of Chitosan Nanoparticles: A Review.” *Processes*, **8** 1173. <https://doi.org/10.3390/pr8091173> (2020)
64. Gafri, HFS, Mohamed Zuki, F, Aroua, MK, Hashim, NA, “Mechanism of Bacterial Adhesion on Ultrafiltration Membrane Modified by Natural Antimicrobial Polymers (Chitosan) and Combination with Activated Carbon (PAC).” *Rev. Chem. Eng.*, **35** 421–443. <https://doi.org/10.1515/revce-2017-0006> (2019)
65. Akbari-Alavijeh, S, Shaddel, R, Jafari, SM, “Nanostructures of Chitosan for Encapsulation of Food Ingredients.” In: Jafari, SM, (ed.), *Biopolymer Nanostructures for Food Encapsulation Purposes*, pp. 381–418. Elsevier (2019). <https://doi.org/10.1016/B978-0-12-815663-6.00014-8>.
66. Kong, M, Chen, XG, Liu, CS, Liu, CG, Meng, XH, Yu, LJ, “Antibacterial Mechanism of Chitosan Microspheres in a Solid Dispersing System Against *E. coli*.” *Colloids Surf. B Biointerfaces*, **65** 197–202. <https://doi.org/10.1016/j.col-surf.2008.04.003> (2008)
67. Tortora, GJ, Funke, BR, Case, CL, *Microbiology*, 12th edn. Artmed, Porto Alegre (2017)
68. Rauch, C, Cherkaoui, M, Egan, S, Leigh, J, “The Bio-physics of Condensation of Divalent Cations into the Bacterial Wall has Implications for Growth of Gram-Positive Bacteria.” *Biochim. Biophys. Acta Biomembr.*, **1859** 282–288 (2017). <https://doi.org/10.1016/j.bbamem.2016.12.002>

Publisher's Note Springer Nature remains neutral with regard to jurisdictional claims in published maps and institutional affiliations.

Springer Nature or its licensor (e.g. a society or other partner) holds exclusive rights to this article under a publishing agreement with the author(s) or other rightsholder(s); author self-archiving of the accepted manuscript version of this article is solely governed by the terms of such publishing agreement and applicable law.